

Theoretical analysis of E - J characteristics in a Bi-2223 silver-sheathed tape

T. Kodama^{a,1}, M. Fukuda^a, S. Nishimura^b, E. S. Otabe^a,
M. Kiuchi^b, T. Kiss^b, T. Matsushita^a, K. Itoh^c

^a Faculty of Computer Science and Systems Engineering, Kyushu Institute of Technology, 680-4 Kawazu, Iizuka 820-8502, Japan

^b Department of Electrical and Electronic Systems Engineering, Graduate School of Information Science and Electrical Engineering, Kyushu University, 6-10-1 Hakozaki, Higashi-ku, Fukuoka 812-8581, Japan

^c National Institute for Materials Science, 1-2-1 Sengen, Tsukuba 305-0047, Japan

Abstract

From an analysis of E - J curves with the aid of the flux creep-flow model, it is found that most of the electric field is caused by the flux creep even in the range of electric field in usual resistive measurement. This result is consistent with the fact that the mechanism of flux creep generally explains various phenomena such as the critical current density, the irreversibility field and so on. On the other hand, it is much easier to use the parameters used in the percolation flow model to describe the E - J characteristics phenomenologically. The two models are compared and it is found that the two models are consistent. This gives a theoretical proof for the parameters of the percolation flow model.

Keywords: E - J characteristics, Bi-2223, flux creep-flow model, percolation flow model

PACS: 74.25.Fy, 74.60.Ge, 74.60.Jg, 74.72.Hs, 85.25.Dq

¹ Corresponding author. Postal address: Department of Computer Science and Electronics, Kyushu Institute of Technology, 680-4 Kawazu, Iizuka 820-8502, Japan
Phone: +81-948-29-7663
Fax: +81-948-29-7683
E-mail address: matusita@cse.kyutech.ac.jp

1 Introduction

The E - J characteristics measured using the resistive measurement can be explained by the flux creep-flow model [1] and the percolation flow model [2]. Both models are based on the flux pinning mechanism with an assumption of a wide distribution of the strength. In the former model the E - J characteristics are determined by the flux creep, a discontinuous flux motion by thermal agitation and the flux flow, a continuous flux motion, by the Lorentz force. In the latter model, the thermally agitated motion of flux lines in Fig. 1(a) is approximated by an equivalent flux flow by making the potential shallow as in Fig. 1(b). However, the latter model cannot be directly applied to the range of a very low electric field, where only the flux creep occurs. Therefore, an extensive percolation flow model was proposed [3], in which the electric field due to the flux creep is also taken into account.

In this paper, the ratio of contribution from the flux flow to the total electric field is estimated for a superconducting multifilamentary Bi-2223 silver-sheathed tape using the flux creep-flow model. It is clarified that most of the electric field is caused by the flux creep even in the range of electric field in usual resistive measurements. It was found that a difference of the attempt frequency of flux bundle between the two models can be explained by a depth of shallowed pinning potential. Moreover, it is clarified that the percolation flow model is consistent with the flux creep-flow model from the comparison between the two models. This gives a theoretical proof for the parameters of the percolation flow model.

2 Experimental

Specimen was a superconducting multifilamentary Bi-2223 silver sheathed tape with 59 filaments prepared by the powder-in-tube method. The width and thickness of the tape were 3.7 mm and 270 μm , respectively. The average width and thickness of superconducting filaments were about 320 μm and 11 μm , respectively. The tape was cut in a length of 4.2 mm for the magnetization measurement. The critical temperature, T_c , was 110 K.

The magnetic relaxation was measured in a magnetic field parallel to the c -axis using a SQUID magnetometer (MPMS-7). The magnetic field of sufficient strength was first applied to the specimen, and then reduced to a certain value, and the relaxation of the magnetic moment was measured. The current density was estimated by the irreversible component of the magnetic moment, and the electric field due to the time variation of magnetic flux distribution was estimated at the edge of the filament. It was assumed that the magnetic flux distribution inside the filament obeys the Bean model.

A four probe method was also conducted to measure the E - J characteristics in a magnetic field parallel to the c -axis. The length of the sample was about 42 mm and the distance between voltage terminals was about 10 mm.

The E - J curves evaluated from the both methods at 70 K are shown in Fig. 2. The range of the electric field by the magnetization measurement is of the order of 10^{-10} V/m and is 6 to 7 orders of magnitude lower than that by resistive measurement.

3 Flux Creep-Flow Model

The observed E - J curves are compared with the theoretical analysis using the flux creep-flow model [1]. According to this model, the E - J characteristics can be calculated when the pinning potential is given:

$$U_0 = \frac{0.835g^2k_B J_{c0}^{1/2}}{(2\pi)^{3/2}B^{1/4}}, \quad (1)$$

where J_{c0} is the virtual critical current density in the creep-free case and g^2 is the number of flux lines in the flux bundle. The magnetic field and temperature dependencies of J_{c0} at low fields are assumed as

$$J_{c0} = A \left[1 - \left(\frac{T}{T_c} \right)^2 \right]^m B^{\gamma-1}, \quad (2)$$

where A , m and γ are pinning parameters. It is assumed that A is distributed as

$$f(A) = K \exp \left[-\frac{(\log A - \log A_m)^2}{2\sigma^2} \right], \quad (3)$$

where A_m is the most probable value, σ^2 is a constant representing the degree of deviation and K is a constant.

The value of g^2 is assumed to be determined so that the critical current density under the flux creep might take on a maximum value [4]. Strictly speaking, g^2 depends on E as well as on B and T . For example, we have $g^2 = 1.39$ at $B = 0.3$ T, $T = 70$ K and $E = 10^{-10}$ V/m. However, this value of g^2 is approximately used as a typical value in the present calculation for simplicity. The details of the calculation are described in [1].

The parameters A_m , m and γ listed in Table 1 are used in the entire ranges of temperature and magnetic field. On the other hand, σ^2 was determined at

each temperature; used values are $\sigma^2 = 0.015, 0.017, 0.02, 0.035, 0.04$ and 0.045 at $T = 40$ K, 50 K, 60 K, 70 K, 80 K and 83 K, respectively.

The calculated results are compared with the experimental results at 70 K in Fig. 2. Similar agreement is obtained also at other temperatures. Thus, it can be said that the flux creep-flow model approximately describes the E - J characteristics in wide ranges of temperature, magnetic field and electric field. This shows that the thermal depinning is the basic mechanism which generally determines the E - J characteristics.

4 Results and Discussion

The dotted lines in Fig. 3 show E - J characteristics in the range of resistive measurements at 77.3 K calculated using the flux creep-flow model. The electric field is composed of the flux creep component and the flux flow component. Figure. 4 shows the ratio of flux flow component to the total electric field. For example, the ratio of the flux flow component is about 1% at 0.01 T. The ratio becomes smaller with decreasing temperature. Hence, the most of electric field is caused by the flux creep in the range of the resistive measurement. This result is consistent with the fact that the mechanism of flux creep generally explains various phenomena such as the critical current density, the irreversibility field and so on.

On the other hand, in the percolation flow model [2] the electric field in this

range is approximately expressed as that due to an equivalent flux flow.

$$\begin{aligned}
E(J) &= \frac{\rho_f}{m'+1} J \left(\frac{J}{J_0} \right)^{m'} \left(1 - \frac{J_{cm}}{J} \right)^{m'+1}; & B < B_{GL} \\
&= \frac{\rho_f}{m'+1} J \left(\frac{J}{J_0} \right)^{m'}; & B = B_{GL} \\
&= \frac{\rho_f}{m'+1} |J_{cm}| \left(\frac{|J_{cm}|}{J_0} \right)^{m'} \left\{ \left(1 + \frac{J}{|J_{cm}|} \right)^{m'+1} - 1 \right\}; & B > B_{GL}
\end{aligned} \quad (4)$$

where m' represents the distribution of J_c , J_{cm} is the minimum J_c , J_0 indicates a half-width of distribution, ρ_f is the flux flow resistivity, and B_{GL} is the magnetic field when $J_{cm} = 0$. The E - J curves can easily be calculated using Eq.(4) when these parameters are determined. This is an advantageous point of the percolation model in comparison with the flux creep-flow model in which a complicated calculation is needed.

However, in the creep region of a very low electric field such as 10^{-10} V/m, the theoretical prediction deviates from experiment due to a part of flux creep which was neglected. Therefore, the extensive percolation flow model was proposed [3]. Since the pinning potential is shallowed by U_1 for activated flux lines, the height of potential barrier which these flux lines feel is ΔU as illustrated in Fig. 1(b). Arrhenius' expression was assumed for the probability for flux lines to overcome the barrier. The electric field due to the flux creep is added to that due to the equivalent flux flow. It is simply assumed that a magnitude of ΔU is proportional to that of J_c . The applicability of this assumption will be argued elsewhere. In addition, the attempt frequency ν_0 is assumed as a fitting parameter and a value of the order of 10^7 Hz is used to explain experimental results at low electric fields [3].

On the other hand, ν_0 can be estimated from

$$\nu_0 = \frac{\rho_f J_{c0}}{a_f B}. \quad (5)$$

Its value is of the order of 10^{10} Hz and is about 3 orders of magnitude higher than that assumed in the extensive percolation flow model. Since the potential barrier is given by $U_1 + \Delta U$ as illustrated in Fig. 1(b), the electric field due to the flux creep is expressed as

$$E = Ba_f \nu_0 \exp\left(-\frac{U_1}{k_B T}\right) \exp\left(-\frac{\Delta U}{k_B T}\right). \quad (6)$$

Then, the new attempt frequency in the extensive percolation flow model is

$$\nu'_0 = \nu_0 \exp\left(-\frac{U_1}{k_B T}\right). \quad (7)$$

This demonstrates that ν'_0 is much smaller than ν_0 . The difference of 3 orders of magnitude can be explained by assuming $U_1/k_B = 534$ K at 77.3 K. This value seems to be reasonable for Bi-2223 superconductor.

Here, the results of the two theoretical models are compared. In the first place, the theoretical E - J curves of the creep-flow model are adjusted to fit the experimental curves. Secondly, the theoretical results of percolation flow model are also adjusted to fit the experimental results. Then, these two theoretical results are compared in Fig. 3. A fairly good agreement was obtained between the two models. Therefore, it can be concluded that the percolation flow model is consistent with the flux creep-flow model. This means that the flux creep-flow model can give a theoretical foundation of the percolation flow model. Namely, J_{cm} , which is merely a fitting parameter in the percolation flow model, can be explained using J_{c0} which can be estimated on the basis of material parameters. The last problem is to check the simple assumption on the proportionality between ΔU and J_{cm} in the range of low electric field.

5 Summary

In this paper E - J characteristics were measured for a superconducting multi-filamentary Bi-2223 silver-sheathed tape in a wide range of electric field. This result was compared with the theoretical results of the flux creep-flow model and the percolation flow model. The following results are obtained.

- (i) It is found that most of the electric field is caused by the flux creep even in the range of the usual resistive measurement. This result is consistent with the fact that the mechanism of flux creep generally explains various phenomena such as the critical current density, the irreversibility field and so on.
- (ii) A difference of the attempt frequency of flux bundle between the flux creep-flow model and the extensive percolation flow model can be explained by a difference of assumed pinning potential.
- (iii) The flux creep-flow model can give a theoretical foundation of the percolation flow model in the electric-field range of usual resistive measurements.

References

- [1] T. Matsushita, T. Tohdoh, N. Ihara, Physica C **259** (1996) 321.
- [2] K. Yamafuji, T. Kiss, Physica C **258** (1996) 197.
- [3] T. Kiss, S. Nishimura, M. Inoue, H. Okamoto, M. Kanazawa, Y. Sumiyoshi, to be published in proceeding of ICMC 2001.
- [4] T. Matsushita, Physica C **217** (1993) 461.

Table 1

Parameters used in numerical calculation.

A_m	m	γ
9.0×10^8	2.0	0.51

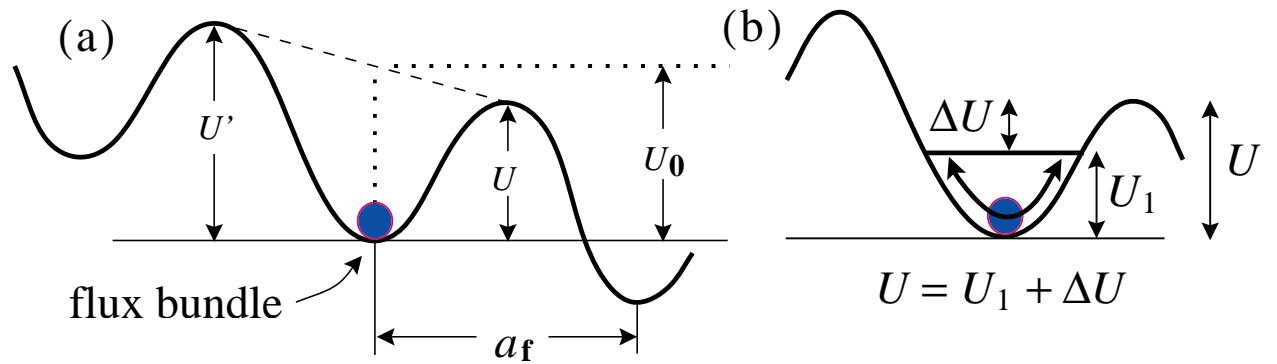


Figure 1: T. Kodama *et al.*/VPP-31/ ISS2001

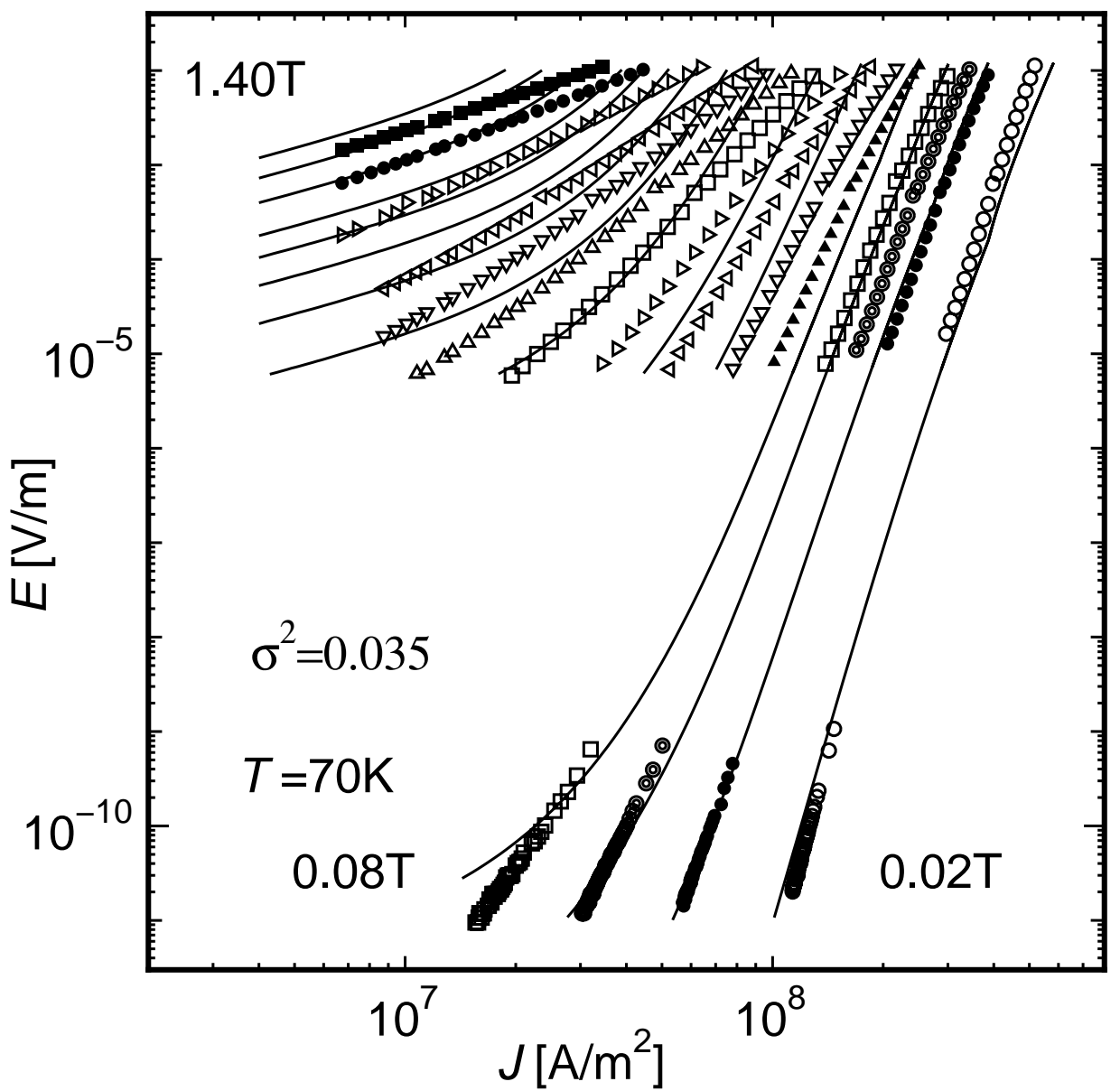


Figure 2: T. Kodama *et al.*/VPP-31/ ISS2001

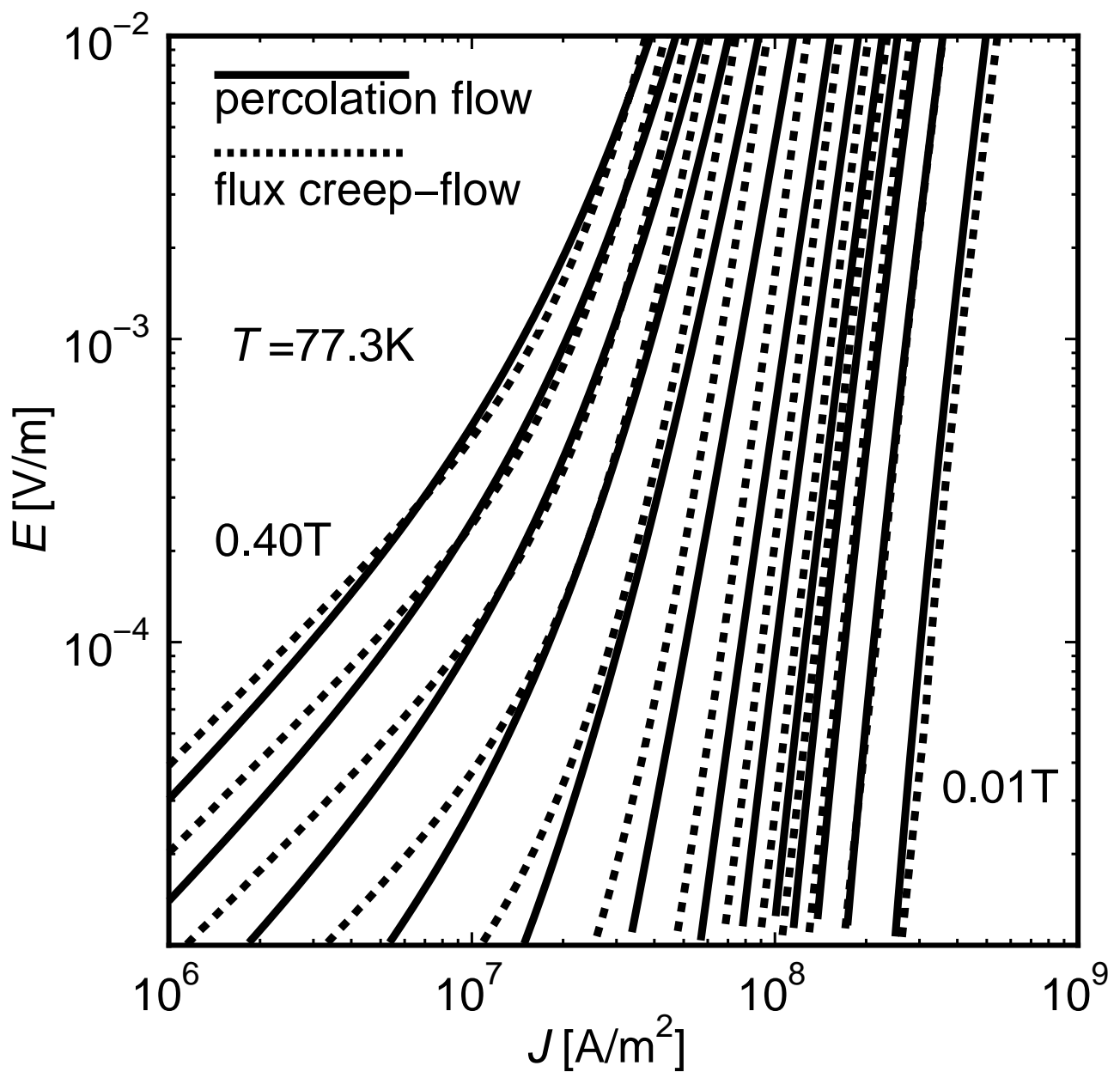


Figure 3: T. Kodama *et al.*/VPP-31/ ISS2001

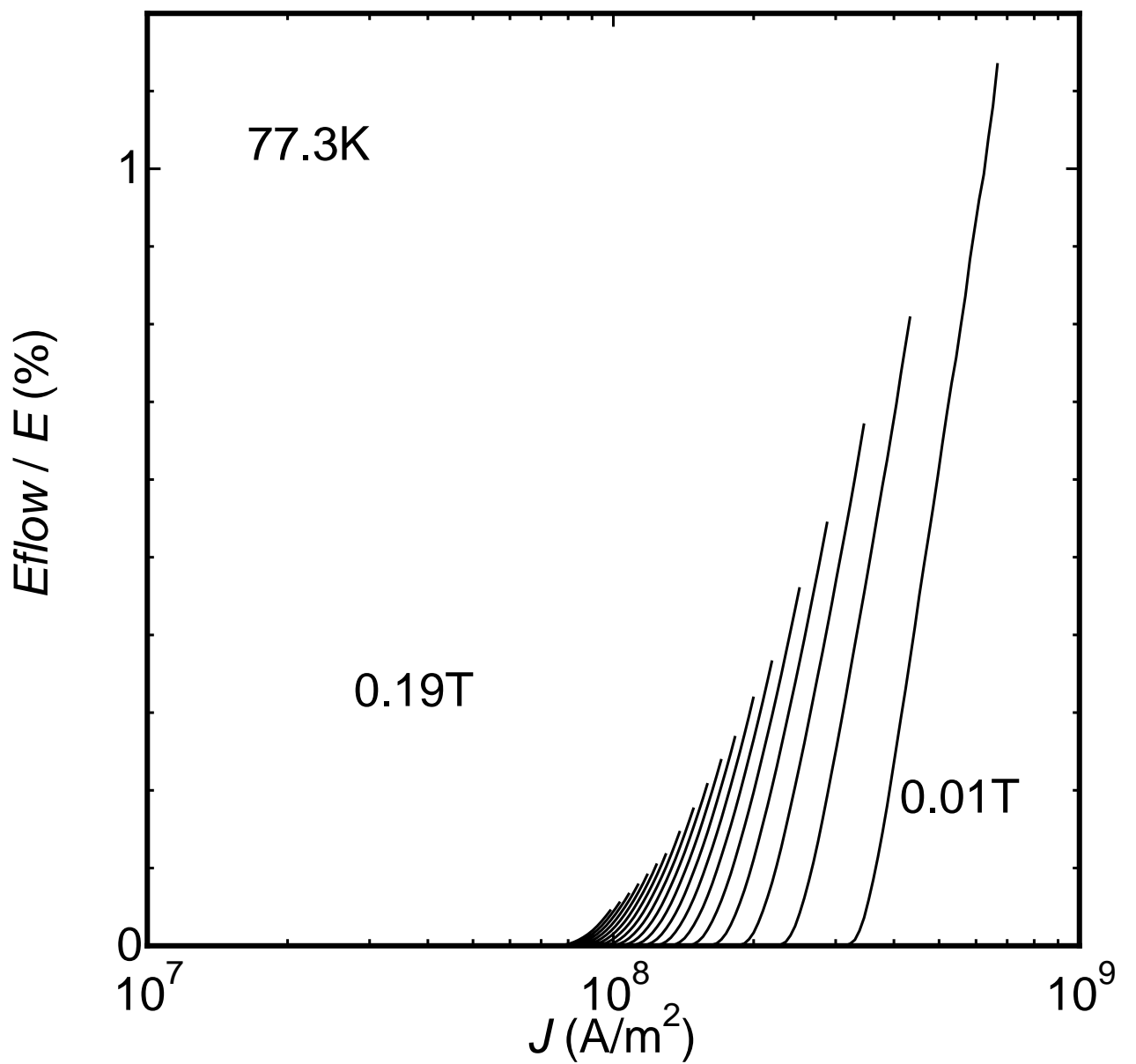


Figure 4: T. Kodama *et al.*/VPP-31/ ISS2001

Figure caption

Fig. 1. (a) Pinning energy of flux bundle vs its position. (b) Pinning potential is regarded to be made shallow by U_1 due to the movement of pinned flux bundle in the percolation model.

Fig. 2. Comparison of E - J curves between experiment (symbols) and theory (lines) at 70 K. Experimental results are obtained by four probe method (top) and the magnetization method (bottom).

Fig. 3. Comparison of E - J theoretical curves between the flux creep-flow model (dotted lines) and the percolation flow model (solid lines) at 77.3 K.

Fig. 4. Ratio of contribution of flux flow to the total electric field predicted by the flux creep-flow model at 77.3 K. Magnetic field is varied from 0.01 T to 0.19 T with a stop of 0.01 T.